

MOL #55111

## **Inverse Effects on Gating and Modulation Caused by a Mutation in the M2-3 Linker of the GABA<sub>A</sub> Receptor Gamma Subunit**

Sean M. O'Shea, Carrie A. Williams, and Andrew Jenkins

Department of Anesthesiology, Emory School of Medicine, Atlanta, GA 30322, USA

Running Title: Mutation Alters Induced and Modulated Receptor Gating

Corresponding author: Dr. Sean M. O'Shea

(Current address) Department of Molecular Neurogenetics  
Max Planck Institute of Biophysics  
Max-von-Laue-Strasse 3  
D-60438 Frankfurt am Main, Germany  
sean.oshea@mpibp-frankfurt.mpg.de

Text Pages: 45, Figures: 6, Tables: 2

Supplemental material: 1 Figure (S1)

Total number of words in Abstract: 250

Introduction: 550

Discussion: 1092

Abbreviations: GABA<sub>A</sub>R, type "A" GABA receptor; WT, wild-type  $\alpha 1\beta 1\gamma 2$  GABA<sub>A</sub>R; MUT, mutant  $\alpha 1\beta 1\gamma 2$ (L278A) GABA<sub>A</sub>R; M2-3 linker, extracellular domain joining transmembrane domains 2 and 3; LGIC, ligand-gated ion channel; PRO, propofol; DMSO, dimethylsulfoxide; HEK, human embryonic kidney; DMEM, Dulbecco's Modified Eagle Medium; FBS, fetal bovine serum; LL, log likelihood;  $\epsilon$ , relative efficacy;  $t_{crit}$ , critical time;  $P_o$ , mean burst open probability; THDOC, tetrahydrodeoxycorticosterone; P4S, piperidine-4-sulfonic acid.

## ABSTRACT

M2-3 linkers are receptor subunit domains known to be critical for the normal function of cys-loop ligand-gated ion channels. Previous studies of  $\alpha$  and  $\beta$  subunits of type “A”  $\gamma$ -aminobutyric acid receptors (GABA<sub>A</sub>Rs) suggest that these linkers couple extracellular elements involved in GABA binding to the transmembrane segments that control the opening of the ion channel. To study the importance of the  $\gamma$  subunit M2-3 linker, we examined the macroscopic and single-channel effects of an engineered  $\gamma 2(L287A)$  mutation on GABA activation and propofol modulation. In the macroscopic analysis, we found that the  $\gamma 2(L287A)$  mutation decreased GABA potency but increased the ability of propofol to enhance both GABA potency and efficacy compared to wild-type receptors. Indeed, while propofol had significant effects on GABA potency in wild-type receptors, we found that propofol produced no corresponding increase in GABA efficacy. At the single-channel level, mutant receptors showed a loss in the longest of three open-time components as compared to wild-type receptors under GABA activation. Furthermore, propofol reduced the duration of one closed-time component, increased the duration of two open-time components and generated a third open component with a longer lifetime in mutant compared to wild-type receptors. Taken together, we conclude that although the  $\gamma$  subunit is not required for the binding of GABA or propofol, the M2-3 linker of this subunit plays a critical role in channel gating by GABA and allosteric modulation by propofol. Our results also suggest that in wild-type receptors, propofol exerts its enhancing effects by mechanisms extrinsic to channel gating.

Despite over 20 years of routine use as an intravenous general anesthetic, the molecular mechanism by which propofol (PRO: 2,6-diisopropyl phenol) produces sedation and unconsciousness remains a mystery. Previous theories proposed that general anesthetics act by nonspecifically disrupting the order of membrane lipids, but it is now widely accepted that PRO exerts its sedative effects through defined amino acids located on the type “A” gamma-aminobutyric acid receptor (GABA<sub>A</sub>R), an inhibitory ligand-gated ion channel (LGIC: Franks and Lieb, 1998; Hemmings et al., 2005). Most compellingly, point mutations that render the GABA<sub>A</sub>R insensitive to enhancement by PRO have been used to produce a genetically-engineered mouse strain that is hyper-resistant to PRO anesthesia (Jurd et al., 2003).

In both native and heterologous expression systems, PRO synergistically enhances submaximal GABA responses, leading to a potentiation in GABAergic function (Hales and Lambert, 1991). At saturating GABA concentrations, PRO does not further enhance peak GABA<sub>A</sub>R responses, but rather prolongs the duration of its time course (Manuel and Davies, 1998; Mody and Pearce, 2004). At present, it is still unclear whether PRO achieves these effects by allosterically increasing GABA binding affinity, enhancing GABA<sub>A</sub>R gating (O'Shea et al., 2000) or by impairing GABA<sub>A</sub>R desensitization (Bai et al., 1999).

GABA<sub>A</sub>Rs are pentameric chloride channels, most commonly composed of 2 $\alpha$ , 2 $\beta$  and one  $\gamma$  subunit (McKernan and Whiting, 1996). GABA binding occurs at extracellular amino acid residues located at  $\alpha/\beta$  interfaces, while PRO binds at amphipathic cavities

that are located between the four transmembrane (M1-M4) helices of  $\beta$  subunits (Bali and Akabas, 2004; Krasowski et al., 1998; Richardson et al., 2007). The proposed GABA and PRO binding sites are connected both to the channel gate and to each other via three N-terminal interacting loops known to disrupt channel gating when mutated (Kash et al., 2003; Kash et al., 2004; Newell and Czajkowski, 2003). Specifically, electrostatic interactions between residues in the M2-M3 linker and these N-terminal loops are proposed to couple agonist binding with channel gating at the pore. In support of this idea, GABA<sub>A</sub>Rs containing  $\gamma 2(K289M)$ , a naturally-occurring M2-M3 linker mutation found in epilepsy (GEFS<sup>+</sup>, Baulac et al., 2001) patients, show decreased channel open times in saturating concentrations of GABA (Bianchi et al., 2002; Hales et al., 2006).

In this study, we further characterized the role of this critical M2-M3 linker region in GABA activation and PRO modulation. Specifically, we used a combination of whole-cell and single-channel electrophysiological techniques to compare the gating reaction kinetics of wild-type  $\alpha 1\beta 1\gamma 2$  and mutant  $\alpha 1\beta 1\gamma 2(L287A)$  GABA<sub>A</sub>Rs in the presence and absence of PRO. This particular strategy was chosen for the following reasons. First, as a neighbor of  $\gamma 2(K289M)$ , the  $\gamma 2(L287A)$  mutation lies in the critical M2-M3 linker region already known to affect channel gating. Second, a previous alanine-scan of the homologous region in the  $\alpha$  subunit showed that the corresponding swap at  $\alpha 2(L277A)$  produced a larger decrease in the GABA EC<sub>50</sub> than the  $\alpha 2(K279A)$  substitution (O'Shea and Harrison, 2000). Third, since the  $\gamma$  subunit is not required for GABA activation (Pritchett et al., 1989), PRO modulation, or PRO direct activation (Jones et al., 1995),

introducing the mutation into the single-copy  $\gamma 2$  subunit should specifically perturb GABA<sub>A</sub>R channel gating without disrupting either GABA or PRO binding. Here, we conclude that the  $\gamma 2$ (L287A) mutation introduced a modest defect in GABA-induced gating that simultaneously increased PRO potentiation.

## MATERIALS AND METHODS

### Cell culture and subunit expression

For whole-cell recordings, human embryonic kidney (HEK) 293 cells were grown on poly-lysine treated coverslips in 35 mM dishes as previously described (Richardson et al., 2007) and maintained in DMEM<sup>+</sup>, containing DMEM (Gibco), L-glutamine (Gibco), 1% penicillin-streptomycin (Gibco) and 5% fetal bovine serum (FBS, Hyclone) at pH 7.4. For single-channel recordings, HEK 293 cells were grown directly on dish surfaces with “low growth” DMEM<sup>+</sup> containing 1% FBS as described by (Lema and Auerbach, 2006).

Human  $\alpha 1$ ,  $\beta 1$  and  $\gamma 2S$  GABA<sub>A</sub>R subunit cDNAs in the pCIS expression vector were generously provided by Neil Harrison (Weill Medical College of Cornell University, New York). The  $\gamma 2S$ (L287A) mutation was introduced using the QuickChange mutagenesis kit (Stratagene) and confirmed by complete dideoxy-sequencing of the insert. Cells were transfected with  $\alpha 1$ ,  $\beta 1$  and  $\gamma 2S$  or  $\gamma 2S$ (L287A) GABA<sub>A</sub>R subunit cDNAs in a 1:1:1 ratio using the calcium phosphate method. For whole-cell recordings, GFP cDNA was added to the transfection mixture to identify positively-transfected cells. For single-

channel recordings, human CD8 surface antigen was used as the marker, and then cells were treated with anti-CD8 antibody-coated Dynabeads (Invitrogen).

### **Whole-cell electrophysiology**

For GABA dose-response curves, GABA<sub>A</sub>R currents were recorded using the whole-cell patch clamp technique as previously described (Richardson et al., 2007). Briefly, cells were voltage-clamped at -60 mV while drugs (GABA and/or PRO) were applied via the extracellular solution using a rapid solution changer. Even though we waited sufficient time for receptors to fully recover between GABA applications, we cannot exclude the effects of fast desensitization before the peak response was reached. Extracellular solution contained (in mM): 145 NaCl, 3 KCl, 1.5 CaCl<sub>2</sub>, 1 MgCl<sub>2</sub>, 6 D-glucose, and 10 HEPES, adjusted to pH 7.4 using KOH. Pipettes were filled with intracellular solution containing (in mM): 145 N-methyl-d-glucamine, 5 K<sub>2</sub>ATP, 1.1 EGTA, 2 MgCl<sub>2</sub>, 5 HEPES and 0.1 CaCl<sub>2</sub>, adjusted to pH 7.2 using KOH.

### **Single-channel electrophysiology**

We recorded single-channel activity using the cell-attached patch configuration as described in Lema and Auerbach (2006). Briefly, data was recorded using a +80 mV pipette potential (~ -100 mV estimated cell membrane potential) and analyzed using QuB software (<http://www.qub.buffalo.edu>). In this configuration, drugs were equilibrated with GABA<sub>A</sub>Rs via the recording pipette for the duration of the experiment.

The bath solution contained (in mM): 140 NaCl, 5 KCl, 1 MgCl<sub>2</sub>, 2 CaCl<sub>2</sub>, 10 glucose, 10 HEPES, pH 7.4. Pipettes were filled with solution containing (in mM): 120 NaCl, 5 KCl, 10 MgCl<sub>2</sub>, 0.1 CaCl<sub>2</sub>, 10 glucose, 10 HEPES, pH 7.4.

## Whole-cell analysis

Dose response curve data was fitted using the following form of the Hill equation with four free parameters:  $((I_{\max} - I_{\min}) * (D^{n_H} / (D^{n_H} + EC_{50}^{n_H})) + I_{\min})$ , where  $I_{\max}$  = the maximal normalized response in saturating GABA,  $I_{\min}$  = the normalized response in the absence of GABA,  $D$  = the GABA concentration,  $n_H$  = the Hill coefficient, and  $EC_{50}$  = the concentration of GABA producing a half-maximal response. All reported values are taken from these parameters, fitted from individual experiments which were then pooled within each condition.

## Overview of single-channel analysis

As described in Lema and Auerbach (2006), we analyzed data files using SKM idealization (Qin, 2004) and MIL fitting (Qin et al., 1996) of kinetic parameters. Note that using these algorithms makes “oversampling” (e.g., sampling faster than the Nyquist theorem) unnecessary, as compared to threshold-based event detection. Therefore, recordings were low-pass filtered at 10 kHz using a 4-pole Bessel filter and digitized at 20 kHz using QuB analysis software ([http: www.qub.buffalo.edu](http://www.qub.buffalo.edu)). Data



were fitted using a 0.15 ms “dead time”, a value that was ~ 2 times faster than the shortest measured time constant.

### Definition of a “burst”

By adapting the method described in Lema and Auerbach (2006), we simplified the interpretation of our single-channel burst analysis by applying a number of conditions and criteria to our definition of a burst. First, to minimize contributions from monoliganded and unliganded closed states to our measurements of gating parameters, we used a saturating concentration of GABA. Second, we applied a variable  $t_{crit}$  to each patch that removed all but the two shortest closed time components from our analysis. This decision was guided by previous determinations that only the two shortest closed-time components are GABA concentration-independent and that burst open probabilities (burst  $P_o$  values) approach their maximum at  $t_{crit}$  values < 20 ms (Newland et al., 1991). Our own experiments using 100  $\mu$ M GABA were in general agreement with these findings, as burst  $P_o$  values at 100  $\mu$ M GABA and 5 mM GABA converged at  $t_{crit}$  values < 20 ms (data not shown). Using this procedure, we effectively removed long-lived desensitized closed states from our estimates of gating (Lema and Auerbach, 2006; Newland et al., 1991) and reduced our window of analysis from clusters (defined using a fixed  $t_{crit}$  of 100 ms per patch) to bursts (defined using a variable  $t_{crit}$  of < 20 ms per patch). Third, we applied a 30 event minimum criterion to our definition of a burst. This criterion allowed us to measure enough intraburst events to extract meaningful kinetic data of the gating reaction (e.g., to observe transitions between multiple open

states), yet still exclude thousands of short-lived, single-opening bursts. By applying these three conditions to our analysis, we were then able to extract meaningful estimates of GABA<sub>A</sub>R “intraburst” gating parameters using models directly fitted from “intraburst” open and closed dwell times.

### **Analysis of a burst**

Supplemental Figure S1 shows a representative analysis of a burst from wild-type  $\alpha 1\beta 1\gamma 2$  GABA<sub>A</sub>Rs equilibrated with 5 mM GABA. We used the QuB AMP function to sort 111 individual events into two conductance classes (closed and open), shown in Supplemental Figure S1A as two Gaussian distributions. Under our experimental conditions, wild-type GABA<sub>A</sub>Rs predominantly open with ~ 2 pA amplitudes. Using this method, low-amplitude classes (e.g., sub-conductance states) were not separately quantified. Supplemental Figure S1B shows the dwell times for each closure within the burst, while Supplemental Figure S1C shows the corresponding open dwell times. Mean values for the closed and open times in this burst were calculated as 1.29 ms and 1.33 ms, respectively. By using the following approximation to calculate the mean burst  $P_o$ , (open time / (open time + closed time)), we calculated a value of 0.51 ( $1.33 / (1.29 + 1.33)$ ) for this individual burst. This analysis was then repeated for all the bursts in this patch, as well as all the patches recorded under the four test conditions (wild-type and mutant GABA<sub>A</sub>Rs with or without PRO).

## Evaluation of Curve Fitting by Log Likelihood

Our decision to use two closed components and up to three open components to fit and model our data is guided by attempts to maximize the log-likelihood of the fit, while using the least number of closed and open time components to adequately describe the data. Previous GABA<sub>A</sub>Rs single-channel studies have observed four closed (C) and two open (O) intraburst components (Mortensen and Smart, 2007), 3C and 3O components (Lema and Auerbach, 2006), 5C and 3O components (Macdonald et al., 1989), and 3C and 3O components (Steinbach and Akk, 2001) when fitting single patches. By using a  $\Delta LL$  cutoff of -10 (Lema and Auerbach, 2006), our aim was to avoid over-parameterization of our data, yet still allow the measurement of rare, long-lived openings. This cutoff is conservative versus other methods that attempt to discriminate between simple and more complex models (Csanady, 2006). In addition to a log-likelihood evaluation of curve fitting, we also performed a manual “reality check” for the fit of each experiment. Fits of the data based on chosen kinetic models were visually inspected for goodness of fit, and fits generating rate constants with near-zero or near-infinite values were re-run with different starting values, or discarded (in the case of unnecessary components), as appropriate.

## Alternate kinetic models

Using QuB software, we calculated that 2 closed (C) and 3 open (O) states can be connected in 98 non-equivalent topologies (15 without loops). Like previous

investigators (Haas and Macdonald, 1999; Jones and Westbrook, 1995; Lema and Auerbach, 2006; Steinbach and Akk, 2001; Weiss and Magleby, 1989), we were unable to distinguish a single “best” model using stationary (equilibrium) kinetic measurements. Therefore, rather than test all possible models using a “brute force” approach on the WT-PRO condition, or simulate macroscopic responses to saturating GABA pulses, we based our kinetic scheme on a recent model that was developed using both of these strategies (Lema and Auerbach, 2006). Compared to Lema and Auerbach’s 6-state “core” (3C, 3O) model, our 5-state (2C, 3O) model topology was identical except for the omission of a “C3” closed state. Since the corresponding long-lived third closed component may contain GABA concentration-dependent closures (Newland et al., 1991), and  $t_{\text{crit}}$  values  $< 20$  ms removed this third closed component, we chose to omit this closed state from our final kinetic models of intraburst gating. Note that including this C3 state in our model slightly increased observed mean burst closed times and decreased the corresponding observed mean burst  $P_o$  values, but did not change the relative trends that we observed and report here in Tables 1 and 2.

## Statistical analysis

Comparison of global single-channel parameters were performed by directly comparing log-likelihood values, while parameters from individual fits were compared at the  $p < 0.05$  significance level with a Student’s unpaired t-test. Dose-response curve parameters (with or without PRO) were taken from responses from the same cell, so results were compared using a Student’s paired t-test at the  $p < 0.05$  significance level.

## Materials

Unless otherwise stated, all reagents were obtained from Sigma.

## RESULTS

### PRO did not increase wild-type maximal responses

Before examining the effects of an M2-M3 linker mutation on the single-channel kinetics of GABA<sub>A</sub>Rs, we began by comparing GABA whole-cell dose response curves under four test conditions: wild-type  $\alpha 1\beta 1\gamma 2$  GABA<sub>A</sub>Rs in the absence of PRO (WT-PRO), wild-type receptors in the presence of PRO (WT+PRO), mutant  $\alpha 1\beta 1\gamma 2$ (L287A) receptors in the absence of PRO (MUT-PRO) and mutant receptors in the presence of PRO (MUT+PRO). In our analysis, we placed a special emphasis on comparing maximal responses at agonist saturation ( $I_{\max}$ ) in each of the four conditions. While such measurements are undoubtedly obscured by rapid desensitization during the agonist application (Colquhoun, 1998; Wagner et al., 2004), we used the  $I_{\max}$  (+PRO) /  $I_{\max}$  (-PRO) ratio at agonist saturation ( $\epsilon$ , relative efficacy) to obtain a rough estimate of the effect of PRO on channel gating (O'Shea and Harrison, 2000; O'Shea et al., 2000). Each cell was tested with and without PRO, and peak responses at each GABA concentration were normalized vs. the  $I_{\max}$ (-PRO) for each cell.

Figure 1A shows a wild-type response to a 2 s application of 300  $\mu$ M GABA. For the WT-PRO condition, peak responses were typically maximal at  $\geq 300$   $\mu$ M GABA. Figure 1B shows the same cell's response to 100  $\mu$ M GABA + 10  $\mu$ M PRO after an 8 s pre-application of 10  $\mu$ M PRO. Before the application of GABA, 10  $\mu$ M PRO directly activated wild-type receptors, producing responses that were  $\sim 20\%$  of  $I_{\max}(-\text{PRO})$ . For the WT+PRO condition, application of 100  $\mu$ M GABA produced maximal peak responses, but  $I_{\max}(+\text{PRO})$  was smaller than  $I_{\max}(-\text{PRO})$  by  $\sim 20\%$ . This decrease in  $I_{\max}$  was likely due to a desensitization of wild-type receptors by PRO before GABA application, since an 8 s pre-application of  $\text{EC}_{20}$  GABA produced the same effect (data not shown). The effects of PRO on pooled GABA dose-response curves are summarized in Figure 1C, while Table 1 provides values pooled from individually-fitted experiments. Compared to the WT-PRO condition, the WT+PRO condition showed a  $\sim 7$ -fold decrease in the GABA  $\text{EC}_{50}$  and a 22% decrease in GABA  $\epsilon$ . Taken together, these experiments yielded two primary findings: first, GABA concentrations  $\geq 300$   $\mu$ M were sufficient to saturate wild-type receptors in both the presence and absence of PRO; and second, 10  $\mu$ M PRO preferentially enhanced sub-maximal GABA responses at wild-type receptors.

### **PRO increased mutant maximal responses**

Next, we tested the whole-cell responses of mutant  $\alpha 1\beta 1\gamma 2(\text{L287A})$  GABA<sub>A</sub>Rs to increasing concentrations of GABA. Figure 1D shows a response to 1000  $\mu$ M GABA, a concentration that typically saturated receptor responses in the MUT-PRO condition.

Compared to the WT-PRO condition, receptors in the MUT-PRO condition showed a ~ 2.5-fold higher GABA  $EC_{50}$  value and a slightly reduced Hill slope (see figure legend), indicating that this mutation produced a slight loss of receptor function. We then tested if PRO could restore wild-type GABA sensitivity to mutant receptors. Figure 1E shows a representative response to 300  $\mu$ M GABA + 10  $\mu$ M PRO, which was saturating in the MUT+PRO condition. In contrast to our results with wild-type receptors, 10  $\mu$ M PRO produced only minimal direct activation (responses were 2% of  $I_{max}(-PRO)$ ). After co-application with a saturating concentration of GABA, the  $I_{max}(+PRO)$  was larger than  $I_{max}(-PRO)$ , indicating that PRO enabled supramaximal GABA responses in mutant receptors. Figure 1F and the figure legend summarize these results: the MUT+PRO condition produced a 40-fold decrease in GABA  $EC_{50}$  and a 76% increase in GABA  $\epsilon$  versus the MUT-PRO condition. We also noted that 10  $\mu$ M PRO did not restore wild-type GABA sensitivity to mutant receptors, but rather overshot the GABA  $EC_{50}$  value in the WT+PRO condition by ~ 2-fold.

In summary, these experiments yielded three major findings. First, we established that concentrations of  $\geq 1$  mM GABA were saturating at mutant receptors in both the presence and absence of PRO. Second, 10  $\mu$ M PRO potentiated all concentrations of GABA at mutant receptors, leading to an increase in GABA  $\epsilon$  and a decrease in the GABA  $EC_{50}$ . Third, we hypothesize that mutant receptors have an enhanced susceptibility to potentiation by PRO, as evidenced by the larger increase in GABA  $\epsilon$  and larger GABA  $EC_{50}$  shift versus wild-type receptors. This susceptibility is probably not due to improved PRO binding, since the  $EC_{50}$  values for PRO direct activation at

mutant receptors ( $30.7 \pm 4.1 \mu\text{M}$ ,  $n=11$ ) was higher than at wild-type receptors ( $20.3 \pm 3.1 \mu\text{M}$ ,  $n=9$ ). Rather, mutant receptors showed a higher Hill coefficient for PRO direct activation ( $4.45 \pm 0.48$ ,  $n=11$ ) than wild-type receptors ( $1.34 \pm 0.13$ ,  $n=9$ ), suggesting an altered effect of PRO on receptor gating. In order to directly test this hypothesis, we analyzed the single-channel responses of receptors in each of the four test conditions.

### **PRO did not affect wild-type intraburst gating**

In our whole-cell experiments, we assume that applications of  $\geq 1 \text{ mM}$  GABA produce full receptor occupancy in each of the four conditions. Therefore, we recorded the single-channel behavior of wild-type  $\alpha 1\beta 1\gamma 2$  receptors equilibrated with  $5 \text{ mM}$  GABA. At agonist saturation, standard receptor activation models (Del Castillo and Katz, 1957) define receptor gating as a continuous and uniform “chatter” (short-lived openings and closures) of receptor activity as the channel oscillates between liganded closed and open states. In the patch shown in Figure 2A, we observed channel openings in the WT-PRO condition as brief,  $\sim 2 \text{ pA}$  upward deflections. Although GABA was present during the entire recording, these openings were not continuous, but separated by both short and long-duration closures.

The long-duration pauses in channel activity are generally defined as desensitization, a receptor state where agonist binding sites are occupied, but the channel is closed (Mortensen and Smart, 2007; Newland et al., 1991). For this patch, we estimate that wild-type channels were inactive (cumulatively) for over 75% of the 20 min recording.



These long-lived closures tended to cluster channel activity, shown at a faster time-scale in Figure 2B. Note that although these clusters were readily apparent in 5 mM GABA, we did not attach any special significance to the duration of these clusters. Therefore, we uniformly applied  $t_{\text{crit}}$  values of 100 ms to each patch to generate segment lists of variable-length clusters, which were then broken down into bursts using variable  $t_{\text{crit}}$  values < 20 ms for final analysis (see Methods).

We also observed that recordings routinely contained activity from multiple channels, shown here by the occasional simultaneous “stacked” openings. To minimize the effects of these simultaneous openings on our measurements, we excluded data segments in which more than 2% of the openings were stacked. The presence of multiple channels in the patch also precluded us from rigorously determining the degree of channel desensitization. Despite this complexity, since desensitized closures are generally considered to be longer than the closures associated with gating, we safely used a  $t_{\text{crit}}$  procedure to remove them from our analysis without affecting our estimates of gating (Lema and Auerbach, 2006). Typically, we found that patches contained at least five closed components with durations > 20 ms (data not shown), but they were not analyzed further in this study.

Figure 2C shows a representative burst displayed at a fast time-scale after the application of  $t_{\text{crit}}$ . In the absence of contamination from unliganded and monoliganded closures (by using saturating agonist concentrations), long-lived desensitized closures (by using  $t_{\text{crit}}$ ), and double openings (by manual deletion from the record), we calculated

an unambiguous measurement of “intra-burst” gating kinetics from the durations of the remaining open and closed dwell times. Table 1 shows the mean channel amplitude, mean burst closed and open times, and mean burst  $P_o$  (open probability within a burst) calculated for multiple bursts pooled from multiple patches. Despite the removal of long-lived (e.g., > 20 ms) closures, the pooled mean burst  $P_o$  for channels in the WT-PRO condition was actually quite low ( $0.53 \pm 0.03$ ).

Figures 2D – 2F show the behavior of wild-type channels in 5 mM GABA + 10  $\mu$ M PRO. When compared to channels in the WT-PRO condition (Figures 2A – 2C), PRO produced no consistent differences in channel activity at agonist saturation shown at either the cluster (Figure 2E) or burst (Figure 2F) level of analysis. When compared to channels in the WT-PRO condition, Table 1 shows that PRO produced no significant effects in the mean channel amplitude, mean burst closed and open times, or mean burst  $P_o$  when pooled from multiple bursts and patches. PRO also produced no significant changes in closed times between clusters when analyzed at low resolution (threshold-based detection at 0.2 kHz digital filtering, data not shown), although the presence of multiple channels in the WT+PRO condition made our desensitization measurements subject to the same caveats previously described for the WT-PRO condition.

## PRO increased mutant intraburst gating

Because of confounding factors in our whole-cell experiments such as desensitization and varying numbers of receptors expressed per cell, we were unable to conclude from normalized GABA  $\varepsilon$  values (Figure 6, legend) or from un-normalized  $I_{\max}$  amplitudes (data not shown) if the  $\gamma 2(L287A)$  mutation impaired receptor gating. To resolve this issue, we next recorded the single-channel behavior of mutant  $\alpha 1\beta 1\gamma 2(L287A)$  receptors equilibrated with 5 mM GABA.

As shown in Figures 3A – 3C and Table 2, the  $\sim 2$  pA openings indicate that mutant receptors open with normal single-channel conductances, and also confirm that the mutant  $\gamma 2(L287A)$  subunits incorporate correctly with the wild-type  $\alpha 1$  and  $\beta 1$  subunit background (Angelotti and Macdonald, 1993). Although not immediately obvious from visually comparing the wild-type receptor burst in Figure 2C with the mutant receptor burst in Figure 3C, Table 1 reveals that on average, bursts in the MUT-PRO condition showed a slightly lower mean burst open time than channels in the WT-PRO condition. Therefore, these results confirmed our hypothesis that the M2-M3 linker mutation produces a moderate GABA gating defect.

Since our macroscopic results suggest that PRO increased the GABA  $\varepsilon$  value in mutant receptors, we also tested whether PRO could also increase the burst  $P_o$  at the single-channel level. Figures 3D – 3F show that 10  $\mu$ M PRO produced remarkable effects on mutant channel behavior in the continued presence of 5 mM GABA. At both cluster

(Figure 3E) and burst (Figure 3F) time-scales, channels in the MUT+PRO condition obviously spent a much higher proportion of time in the open state than channels in the MUT-PRO condition. In data pooled from multiple bursts and multiple patches (Table 1), the MUT+PRO condition showed an increased mean burst open time and mean burst  $P_o$ , a decreased mean burst closed time, and an unchanged mean channel amplitude when compared to the MUT-PRO condition. We also noticed that, in agreement with our whole-cell comparisons of relative efficacy (GABA  $\epsilon$ , Figure 6 legend), the mean burst  $P_o$  (Table 1) of the MUT+PRO condition was higher than in the WT+PRO condition, suggesting that mutant receptors have a higher “ceiling” for potentiation than wild-type receptors. Since the mean burst  $P_o$  of receptors in the WT-PRO condition was low enough ( $0.54 \pm 0.05$ ) to accommodate potentiation, we were intrigued as to why wild-type receptors did not show a similar increase in mean burst  $P_o$ . As a result, we continued our investigation into the mechanistic aspects of GABA<sub>A</sub>R gating kinetics.

### **PRO enabled “high- $P_o$ ” gating in mutants**

As reported in other GABA<sub>A</sub>R investigations using various preparations and subunit combinations (Keramidas et al., 2006; Lema and Auerbach, 2006; Newland et al., 1991), we observed that some patches in the WT-PRO condition showed clear “modes” of channel activity. In our experiments, 3 of 8 patches in the WT-PRO condition had channel bursting behavior that was easily separable into multiple modes, but the appearance and transitions between those modes appeared to be random.

Figure 4 shows the distribution of burst  $P_o$  values pooled from multiple bursts and multiple patches within each of the four conditions. After plotting the number of bursts observed in 0.05- $P_o$  width bins, the histogram revealed that channels in the WT-PRO condition showed major modes of activity centered at 0.40-0.45 and 0.70-0.75  $P_o$  (Figure 4A). In comparison, channels in the WT+PRO condition showed a major mode centered at 0.50-0.55 and a minor one centered at 0.80-0.85  $P_o$ . In the MUT-PRO condition, we observed a single mode centered at 0.35-0.40  $P_o$  (Figure 5B), while channels in the MUT+PRO condition showed a minor mode centered at 0.40-0.45 and a major one centered at 0.95-1.00.

Since the number of modes and the underlying cause of this modal activity in GABA<sub>A</sub>Rs was unknown, we arbitrarily categorized bursts into “high- $P_o$ ” and “low- $P_o$ ” gating modes using a  $P_o$  value of 0.70. To a first approximation, PRO increased the normalized percentage of high- $P_o$  bursts in mutant (MUT-PRO, 8%; MUT+PRO, 87%) but not wild-type receptors (WT-PRO, 29%; WT+PRO, 26%). Furthermore, it appears that PRO enabled a 0.95-1.00  $P_o$  gating mode in the MUT+PRO condition that was never observed in the MUT-PRO condition, and only rarely observed in the WT-PRO and WT+PRO conditions.

## **PRO increased mutant intraburst open times**

We also tested if PRO had subtle effects on the relative distributions of subpopulations of channel dwell times (e.g., specific kinetic components) that were not reflected in the channel mean open and closed times. As shown in closed time histograms and curve fits (solid lines) including components (dotted lines), two closed components were required to adequately fit data from a patch in the WT-PRO condition (Figure 5A, gray lines) and a patch in the WT+PRO condition (Figure 5A, black lines). For this patch, the two closed components had 0.5 ms and 1.7 ms durations in the absence of PRO, the 1.7 ms component had the larger area, and both components were unchanged by the addition of PRO. In Figure 5C, three open components were required to adequately fit the open time histograms of a patch in the WT-PRO condition. The open components had durations of 0.8 ms, 2.4 ms and 7.3 ms, and the 2.4 ms component had the largest area. As with the closed components, the addition PRO did not change these open components in wild-type receptors.

In contrast, PRO had multiple effects on the open and closed time components of mutant receptors. Figure 5B shows that two closed components were required to fit data from patches in the MUT-PRO and MUT+PRO conditions. In the absence of PRO, the two closed components had 0.6 ms and 2.2 ms durations, with the 2.2 ms component having the largest area, but in the presence of PRO, the second component was shortened to 0.9 ms, and the areas of the two components were roughly equal. In Figure 5D, only two open components were required to fit the MUT-PRO patch, but

three components were necessary to fit the MUT+PRO patch. In the absence of PRO, the open components had 0.8 ms and 1.9 ms durations, while the 0.8 ms component had the largest area. In the presence of PRO, the open components had 1.1 ms, 5.0 ms and 23.4 ms durations, and the 23.4 ms component had the largest area.

As summarized in Table 2, the primary effect of PRO on data pooled from multiple patches containing mutant receptors was to lengthen the durations of two existing open components, to re-introduce a third open component, and to increase the area of a 25 ms time component. To a lesser extent, PRO also shortened the duration of a 1.9 ms closed time component to 1.2 ms in mutant receptors. Taken together, these findings provide a detailed description of how PRO potentiates mutant receptor gating, and further support our conclusion that “intraburst” wild-type receptor gating is unaffected by PRO.

### **Modeling and simulation reveals two GABA<sub>A</sub>R activation pathways**

As detailed in the Methods, we used QuB software to generate kinetic schemes (Figure 6A) and simulations of single-channel activation during our global fitting of data pooled within each of the four conditions. We based our model topology on previously-published schemes for wild-type  $\alpha 1\beta 1\gamma 2$  GABA<sub>A</sub>Rs (Lema and Auerbach, 2006) with the omission of a third long-lived closed state that was deemed unnecessary by comparison of log-likelihood (LL) values and visual inspection of our fits. These models

assume equilibration with saturating concentrations of GABA and therefore do not include desensitized or sub-liganded closed states.

Interestingly, our five-state model for wild-type GABA<sub>A</sub>R gating suggests two alternate GABA activation pathways. The top branch (C1-C2-O1) proceeds directly towards an opening after transition through two agonist-bound closed states, while the bottom branch (C1-C2-O2-O3) proceeds to two interconnected open states. One might intuitively expect that the lower branch (with more open states) would produce a higher burst  $P_o$ . However, when we simulated the two pathways separately, we found that the higher pathway produced a “burst”  $P_o$  of 0.46, while the lower pathway produced a “burst”  $P_o$  of 0.48. When both pathways were simulated together, the simulated “burst”  $P_o$  increased to 0.64, as receptors freely hopped between the upper and lower pathways before eventually dwelling in long-lived closures. Due to the innate connectivity between these two pathways, and the similarity of the time constants between them, we could not detect clear transitions between different modes of gating, as has been reported with other LGICs (Lema and Auerbach, 2006; Newland et al., 1991; Popescu and Auerbach, 2003).

To better understand the role the  $\gamma 2(L287A)$  mutation plays in GABA-induced gating, we compared the models and rate constants generated for the WT-PRO and MUT-PRO conditions. With the exception of the O3 state, the two conditions were well fit using identical state topologies. Since addition of the O3 state in the MUT-PRO condition produced either near-zero or near-infinite rate constants, we assumed that this state



was undetectable to our analysis. This missing O3 state causes receptors that activate by the lower activation pathway to prematurely close versus receptors in the WT-PRO condition, which occasionally make O2 to O3 transitions before closing. Of the remaining rate constants, the mutation had the largest effect on the C2 to O1 rate constant ( $625\text{ s}^{-1}$  to  $232\text{ s}^{-1}$ ). In the upper activation pathway, this 2.7-fold decrease contributes to the modest decrease in mean burst open time that we observed in our single-channel experiments.

Next, we compared the effects of PRO in wild-type and mutant receptors. Consistent with its lack of effect on any of the intraburst closed or open time components, the WT+PRO condition produced only modest ( $< 1.4$ -fold) changes in the individual rate constants compared to the WT-PRO condition. In contrast, the MUT+PRO condition showed a 10.9-fold decrease in the O2 to C2 transition ( $1352\text{ s}^{-1}$  to  $124\text{ s}^{-1}$ ) and the reappearance of the O3 open state. By blocking this “escape route” for receptors that favor the lower activation pathway, PRO effectively traps receptors in O2 and O3, leading to longer mean open times and higher burst  $P_o$  values in single-channel experiments and higher GABA  $\varepsilon$  values in whole-cell experiments. Indeed, after correcting for the differing overall open occupancies, our simulations suggest that while receptors in the WT+PRO condition show a 1.2-fold preference for the upper pathway, receptors in the MUT+PRO condition show a  $> 50$ -fold preference for the lower pathway.

In order to present a more intuitive description of the effect of the mutation on receptor activation and modulation, we constructed a stacked histogram that represents the simulated fractional occupancies for the open states calculated from these models and rate constants (Figure 6B). We should emphasize that due to the branched topologies of the kinetic schemes, calculation of the relationships between the simulated fractional occupancies of each open state and the fitted fractional areas of each open component can be complex. Notwithstanding these complexities, comparing the WT-PRO with the MUT-PRO condition revealed that the mutation increased the fractional occupancy of the O2 state at the expense of the O1 and O3 states, with no occupancy of the O3 state. In comparing the summed fractional occupancies, we also observed that the mutant produced a 1.6-fold reduction in the overall open occupancy versus wild-type receptors.

While PRO had negligible effects on the fractional and overall open-state occupancies of wild-type receptors, PRO produced large changes in the open-state occupancies of receptors in the MUT+PRO compared to the MUT-PRO condition. Specifically, receptors in the MUT+PRO condition showed a reduced fractional occupancy of the O1 state, increased fractional occupancies of the O2 and O3 states, and an increased overall open occupancy compared to the MUT-PRO condition. Given that the mean burst  $P_o$  values in Table 1 represent unweighted mean values pooled from multiple experiments, our simulated values for overall open occupancies are in relatively good agreement with the trends we observed in our experimental data.

Finally, to relate the changes in rate constants from our single-channel experiments to our whole-cell dose response curves, we simulated the macroscopic responses in the absence of desensitization. Specifically, we used each of the four kinetic schemes shown in Figure 6A with two sequential GABA binding steps attached to C1 (Lema and Auerbach, 2006) to simulate whole-cell dose response curves. For the purposes of the simulations, we also assumed that neither the mutation nor PRO altered the GABA binding affinity (GABA  $K_D$ ). Qualitatively, our simulations successfully predicted the trends (Figure 6, legend), but not the values or fold-shifts we observed in our whole-cell experiments (Figure 1, legend). Compared to the WT-PRO condition, the MUT-PRO condition produced a 1.4-fold increase in the simulated GABA  $EC_{50}$ . In wild-type receptors PRO produced no changes, but in mutant receptors PRO decreased the simulated GABA  $EC_{50}$  by 4.6-fold. In our actual whole-cell experiments, GABA  $EC_{50}$  values were increased by 2.5 fold (MUT-PRO vs. WT-PRO), 7-fold (WT+PRO vs. WT-PRO) and 40-fold (MUT+PRO vs. MUT-PRO), respectively, indicating that without the effects on desensitization and GABA binding, our predicted shifts fall significantly short of our experimentally-determined shifts. Similar comparisons of GABA  $\epsilon$  values suggest that our simulations overestimated the effects of PRO on wild-type and mutant receptors versus what we observed in our whole-cell experiments. Therefore, we fully acknowledge the important role processes like desensitization play in GABA<sub>A</sub>R modulation by PRO (Bai et al., 1999) and the shaping of GABAergic synaptic responses (Bianchi and Macdonald, 2002; Jones and Westbrook, 1995). Based on these simulations, we also suggest that PRO primarily potentiates wild-type receptors by

altering GABA binding and / or desensitization, while PRO has an additional synergistic effect on GABA-induced gating in mutant receptors carrying a  $\gamma 2$ (L287A) mutation.

## DISCUSSION

We have measured the effect of a mutation in the GABA<sub>A</sub> receptor  $\gamma 2$  subunit M2-3 linker on receptor gating by GABA and modulation by the general anesthetic PRO. The importance of this region in GABA-mediated channel gating has been clearly demonstrated previously in  $\alpha$  and  $\beta$  subunits (Jones et al., 1995). The goal of this study was to better understand the role the homologous domain plays in the  $\gamma 2$  subunit. Since M2-3 linker residues in  $\gamma$  subunits are unlikely to contribute to either GABA or PRO binding sites, we focused our analysis on the allosteric effects produced by the mutation. Overall, we found that the  $\gamma 2$ (L287A) mutation had modest negative effects on channel gating but strong positive effects on PRO modulation. We will discuss these findings in terms of understanding receptor-gating defects and drug action on LGICs.

When we compared the activation of wild-type and  $\gamma 2$ (L287A) mutant receptors by GABA, we found that the 2.5-fold increase in GABA EC<sub>50</sub> of the mutant receptor was accompanied by a 1.9-fold decrease in mean open time. This decrease was underpinned by a 2.4-fold increase in fractional area of the shortest (0.7 ms) open time and the disappearance of the longest-lived (8 ms) open component. Our results suggest that the  $\gamma 2$ (L287A) mutation produces an impairment of receptor function that can be described as a “low efficacy” condition (Bianchi and Macdonald, 2003) or a “loss

of function” perturbation (Wang et al., 1997). We discounted any effect the mutation may have had on GABA binding since the  $\gamma$  subunit is not required for GABA activation ( $\alpha\beta$  receptors, Jones et al., 1995).

The “loss of function” perturbation induced by the  $\gamma 2$ (L287A) mutation is consistent with previous studies of M2-3 linker function. At homologous and neighboring positions in the  $\alpha$  subunit, the  $\alpha 2$ (L277A) and  $\alpha 2$ (K279A) mutations produced 51-fold and 4-fold increases in the GABA  $EC_{50}$ , respectively (O'Shea and Harrison, 2000). Receptors containing  $\alpha 1$ (K279D) subunits showed a 10-fold decrease in the GABA  $EC_{50}$  (Kash et al., 2003). Lysine-to-methionine (K-to-M) substitutions produced subtler effects on the GABA  $EC_{50}$ , depending on whether the substitution was introduced into  $\alpha 1$  (K278M: 4-fold),  $\beta 2$  (K279M: 5.2-fold), or the  $\gamma 2$  subunit (K289M: no effect, Hales et al., 2006; but also see Bianchi et al., 2002 and Krivoshein and Hess, 2006). Taken together, these findings suggest that all five M2-3 linkers function in unison as a “hinge” region that allosterically transduces energy from agonist binding at the extracellular domains into channel opening at the transmembrane domains (Kash et al., 2003). In our current study, the loss of coupling efficiency introduced at a single locus was sufficient to impair channel gating, even though the  $\gamma 2$ (L287A) mutation was not located within an agonist binding subunit. In agreement with studies of the neighboring  $\gamma 2$ (K289M) mutation (Bianchi et al., 2002; Hales et al., 2006; Krivoshein and Hess, 2006), we observed that the  $\gamma 2$ (L287A) mutation resulted in the loss or reduction of the most stable long-lived openings at the single-channel level, with effects that were more pronounced than the naturally-occurring substitution.

We then tested whether PRO could restore wild-type function to mutant receptors. Surprisingly, when we compared the actions of 10  $\mu$ M PRO on wild-type and mutant receptors we found that the resulting decrease in GABA  $EC_{50}$  was much larger in mutant receptors (~ 40-fold) versus wild-type receptors (~ 7-fold). This larger enhancement was accompanied by a 76% increase in the GABA  $\varepsilon$  value that was not observed in wild-type receptors. At the single-channel level, PRO increased the mean burst  $P_o$  of mutant receptors by 1.7-fold through a 1.9-fold decrease in the mean burst closed time and a 5.8-fold increase in the mean burst open time. Specifically, PRO produced a 1.6-fold decrease in the longer 1.9 ms closed time component, 1.6-fold and 2.8-fold increases in the two shortest open time components, and produced the appearance of a predominant ~ 25 ms open time component that was not detected in the MUT-PRO condition. In summary, not only did PRO introduce “high-efficacy” gating to mutant receptors, it appeared to stabilize a “high- $P_o$ ” mode that was rarely observed in wild-type receptors.

Previous whole-cell studies have used supramaximal enhancements by allosteric modulators to reveal “low efficacy” agonist-receptor combinations. For example, O'Shea et al. (2000) use PRO to decrease the  $EC_{50}$  and increase the  $\varepsilon$  value of the partial agonist piperidine-4-sulfonic acid (P4S) in wild-type  $\alpha 1\beta 1\gamma 2$  GABA<sub>A</sub>Rs. In another example, Krivoshein and Hess (2006) used the barbiturate phenobarbital to decrease  $EC_{50}$  and increase the  $\varepsilon$  value of GABA at  $\alpha 1\beta 2\gamma 2$ (K289M) GABA<sub>A</sub>Rs. Finally, Bianchi and Macdonald (2003) used the neurosteroid tetrahydrodeoxycorticosterone (THDOC)

to increase the  $\varepsilon$  value of GABA at  $\alpha 1\beta 3\delta$  GABA<sub>A</sub>Rs and of  $\beta$ -alanine at  $\alpha 1\beta 3\gamma 2$  GABA<sub>A</sub>Rs.

While PRO potentiated the responses of mutant receptors at all GABA concentrations, saturated responses of wild-type receptors proved to be resistant to further enhancement. Specifically, receptors in the WT+PRO condition showed no increase in GABA  $\varepsilon$  at the whole-cell level, and no increase in the mean burst  $P_o$  at the single-channel level. Since PRO produced no detectable changes in the intraburst kinetics (gating), we necessarily conclude that PRO acts at extraburst closures (desensitization) and / or at GABA binding steps that we could not observe at GABA saturation. Unfortunately, our multichannel patches did not allow us to distinguish between these possibilities in either mutant or wild-type receptors. In mutant receptors, our simulations (Figure 6, legend) indicated these additional potentiation mechanisms undoubtedly complement the effects of PRO that we observed on channel gating.

Mutations in the M2-3 linker region of several cys-loop receptors have been associated with disease states. For instance, in GABA<sub>A</sub>Rs, naturally-occurring M2-3 linker substitutions disrupt normal GABA<sub>A</sub>R function in humans with a hereditary form of epilepsy (GEFS+, Baulac et al., 2001). In addition, M2-3 linker substitutions in glycine receptor subunits produce hereditary hyperekplexia (Rajendra et al., 1994), and M2-3 linker substitutions in nicotinic acetylcholine receptor produce channel-form myasthenia gravis (Sine et al., 1995). The increased sensitivity of M2-3 linker mutants to potentiation by some positive allosteric modulators, as shown in this study and others

(e.g., phenobarbital, Krivoshein and Hess, 2006; THDOC, Bianchi and Macdonald, 2003; PRO, O'Shea and Harrison, 2000 and this study), suggests that low doses of positive allosteric modulators may be an effective treatment for diseases that at least partially target these “low efficacy” synapses. For instance, subanesthetic doses of PRO have been used to temporarily reverse the neurologic effects of hyperekplexia in a transgenic mouse model of the disease (O'Shea et al., 2004). Therefore, understanding the function of LGIC M2-3 linkers and the mechanism of allosteric modulation offers hope for designing treatment strategies for “low-efficacy” channelopathies.

## **ACKNOWLEDGEMENTS**

The authors would like to thank Anthony Auerbach for support during the initial stages of this investigation.



## REFERENCES

- Angelotti TP and Macdonald RL (1993) Assembly of GABA<sub>A</sub> receptor subunits: alpha 1 beta 1 and alpha 1 beta 1 gamma 2S subunits produce unique ion channels with dissimilar single-channel properties. *J Neurosci* **13**:1429-40.
- Bai D, Pennefather PS, MacDonald JF and Orser BA (1999) The general anesthetic propofol slows deactivation and desensitization of GABA(A) receptors. *J Neurosci* **19**:10635-46.
- Bali M and Akabas MH (2004) Defining the propofol binding site location on the GABA<sub>A</sub> receptor. *Mol Pharmacol* **65**:68-76.
- Baulac S, Huberfeld G, Gourfinkel-An I, Mitropoulou G, Beranger A, Prud'homme JF, Baulac M, Brice A, Bruzzone R and LeGuern E (2001) First genetic evidence of GABA(A) receptor dysfunction in epilepsy: a mutation in the gamma2-subunit gene. *Nat Genet* **28**:46-8.
- Bianchi MT and Macdonald RL (2002) Slow phases of GABA(A) receptor desensitization: structural determinants and possible relevance for synaptic function. *J Physiol* **544**:3-18.
- Bianchi MT and Macdonald RL (2003) Neurosteroids shift partial agonist activation of GABA(A) receptor channels from low- to high-efficacy gating patterns. *J Neurosci* **23**:10934-43.
- Bianchi MT, Song L, Zhang H and Macdonald RL (2002) Two different mechanisms of disinhibition produced by GABA<sub>A</sub> receptor mutations linked to epilepsy in humans. *J Neurosci* **22**:5321-7.

- Colquhoun D (1998) Binding, gating, affinity and efficacy: the interpretation of structure-activity relationships for agonists and of the effects of mutating receptors. *Br J Pharmacol* **125**:924-47.
- Csanady L (2006) Statistical evaluation of ion-channel gating models based on distributions of log-likelihood ratios. *Biophys J* **90**:3523-45.
- Del Castillo J and Katz B (1957) Interaction at end-plate receptors between different choline derivatives. *Proc R Soc Lond B Biol Sci* **146**:369-81.
- Franks NP and Lieb WR (1998) Which molecular targets are most relevant to general anaesthesia? *Toxicol Lett* **100-101**:1-8.
- Haas KF and Macdonald RL (1999) GABA<sub>A</sub> receptor subunit gamma2 and delta subtypes confer unique kinetic properties on recombinant GABA<sub>A</sub> receptor currents in mouse fibroblasts. *J Physiol* **514 ( Pt 1)**:27-45.
- Hales TG, Deeb TZ, Tang H, Bollan KA, King DP, Johnson SJ and Connolly CN (2006) An asymmetric contribution to gamma-aminobutyric type A receptor function of a conserved lysine within TM2-3 of alpha1, beta2, and gamma2 subunits. *J Biol Chem* **281**:17034-43.
- Hales TG and Lambert JJ (1991) The actions of propofol on inhibitory amino acid receptors of bovine adrenomedullary chromaffin cells and rodent central neurones. *Br J Pharmacol* **104**:619-28.
- Hemmings HC, Jr., Akabas MH, Goldstein PA, Trudell JR, Orser BA and Harrison NL (2005) Emerging molecular mechanisms of general anesthetic action. *Trends Pharmacol Sci* **26**:503-10.

- Jones MV, Harrison NL, Pritchett DB and Hales TG (1995) Modulation of the GABA<sub>A</sub> receptor by propofol is independent of the gamma subunit. *J Pharmacol Exp Ther* **274**:962-8.
- Jones MV and Westbrook GL (1995) Desensitized states prolong GABA<sub>A</sub> channel responses to brief agonist pulses. *Neuron* **15**:181-91.
- Jurd R, Arras M, Lambert S, Drexler B, Siegwart R, Crestani F, Zaugg M, Vogt KE, Ledermann B, Antkowiak B and Rudolph U (2003) General anesthetic actions in vivo strongly attenuated by a point mutation in the GABA(A) receptor beta3 subunit. *FASEB J* **17**:250-2.
- Kash TL, Jenkins A, Kelley JC, Trudell JR and Harrison NL (2003) Coupling of agonist binding to channel gating in the GABA(A) receptor. *Nature* **421**:272-5.
- Kash TL, Kim T, Trudell JR and Harrison NL (2004) Evaluation of a proposed mechanism of ligand-gated ion channel activation in the GABA<sub>A</sub> and glycine receptors. *Neurosci Lett* **371**:230-4.
- Keramidas A, Kash TL and Harrison NL (2006) The pre-M1 segment of the alpha1 subunit is a transduction element in the activation of the GABA<sub>A</sub> receptor. *J Physiol* **575**:11-22.
- Krasowski MD, Koltchine VV, Rick CE, Ye Q, Finn SE and Harrison NL (1998) Propofol and other intravenous anesthetics have sites of action on the gamma-aminobutyric acid type A receptor distinct from that for isoflurane. *Mol Pharmacol* **53**:530-8.

- Krivoshein AV and Hess GP (2006) On the mechanism of alleviation by phenobarbital of the malfunction of an epilepsy-linked GABA(A) receptor. *Biochemistry* **45**:11632-41.
- Lema GM and Auerbach A (2006) Modes and models of GABA(A) receptor gating. *J Physiol* **572**:183-200.
- Macdonald RL, Rogers CJ and Twyman RE (1989) Kinetic properties of the GABA<sub>A</sub> receptor main conductance state of mouse spinal cord neurones in culture. *J Physiol* **410**:479-99.
- Manuel NA and Davies CH (1998) Pharmacological modulation of GABA(A) receptor-mediated postsynaptic potentials in the CA1 region of the rat hippocampus. *Br J Pharmacol* **125**:1529-42.
- McKernan RM and Whiting PJ (1996) Which GABA<sub>A</sub>-receptor subtypes really occur in the brain? *Trends Neurosci* **19**:139-43.
- Mody I and Pearce RA (2004) Diversity of inhibitory neurotransmission through GABA(A) receptors. *Trends Neurosci* **27**:569-75.
- Mortensen M and Smart TG (2007) Single-channel recording of ligand-gated ion channels. *Nat Protoc* **2**:2826-41.
- Newell JG and Czajkowski C (2003) The GABA<sub>A</sub> receptor alpha 1 subunit Pro174-Asp191 segment is involved in GABA binding and channel gating. *J Biol Chem* **278**:13166-72.
- Newland CF, Colquhoun D and Cull-Candy SG (1991) Single channels activated by high concentrations of GABA in superior cervical ganglion neurones of the rat. *J Physiol* **432**:203-33.

- O'Shea SM, Becker L, Weiher H, Betz H and Laube B (2004) Propofol restores the function of "hyperekplexic" mutant glycine receptors in *Xenopus* oocytes and mice. *J Neurosci* **24**:2322-7.
- O'Shea SM and Harrison NL (2000) Arg-274 and Leu-277 of the gamma-aminobutyric acid type A receptor alpha 2 subunit define agonist efficacy and potency. *J Biol Chem* **275**:22764-8.
- O'Shea SM, Wong LC and Harrison NL (2000) Propofol increases agonist efficacy at the GABA(A) receptor. *Brain Res* **852**:344-8.
- Popescu G and Auerbach A (2003) Modal gating of NMDA receptors and the shape of their synaptic response. *Nat Neurosci* **6**:476-83.
- Pritchett DB, Sontheimer H, Shivers BD, Ymer S, Kettenmann H, Schofield PR and Seeburg PH (1989) Importance of a novel GABA<sub>A</sub> receptor subunit for benzodiazepine pharmacology. *Nature* **338**:582-5.
- Qin F (2004) Restoration of single-channel currents using the segmental k-means method based on hidden Markov modeling. *Biophys J* **86**:1488-501.
- Qin F, Auerbach A and Sachs F (1996) Estimating single-channel kinetic parameters from idealized patch-clamp data containing missed events. *Biophys J* **70**:264-80.
- Rajendra S, Lynch JW, Pierce KD, French CR, Barry PH and Schofield PR (1994) Startle disease mutations reduce the agonist sensitivity of the human inhibitory glycine receptor. *J Biol Chem* **269**:18739-42.
- Richardson JE, Garcia PS, O'Toole KK, Derry JM, Bell SV and Jenkins A (2007) A conserved tyrosine in the beta2 subunit M4 segment is a determinant of gamma-

aminobutyric acid type A receptor sensitivity to propofol. *Anesthesiology* **107**:412-8.

Sine SM, Ohno K, Bouzat C, Auerbach A, Milone M, Pruitt JN and Engel AG (1995)

Mutation of the acetylcholine receptor alpha subunit causes a slow-channel myasthenic syndrome by enhancing agonist binding affinity. *Neuron* **15**:229-39.

Steinbach JH and Akk G (2001) Modulation of GABA(A) receptor channel gating by pentobarbital. *J Physiol* **537**:715-33.

Wagner DA, Czajkowski C and Jones MV (2004) An arginine involved in GABA binding and unbinding but not gating of the GABA(A) receptor. *J Neurosci* **24**:2733-41.

Wang HL, Auerbach A, Bren N, Ohno K, Engel AG and Sine SM (1997) Mutation in the M1 domain of the acetylcholine receptor alpha subunit decreases the rate of agonist dissociation. *J Gen Physiol* **109**:757-66.

Weiss DS and Magleby KL (1989) Gating scheme for single GABA-activated Cl<sup>-</sup> channels determined from stability plots, dwell-time distributions, and adjacent-interval durations. *J Neurosci* **9**:1314-24.

## FOOTNOTES

This work was supported by the National Institutes of Health (GM073959)

Reprint requests: Dr. Andrew Jenkins

Departments of Pharmacology and Anesthesiology

Emory University School of Medicine

Rollins Research Center #5013

1510 Clifton Rd NE

Atlanta GA 30322-3090

Email: [ajenki2@emory.edu](mailto:ajenki2@emory.edu)

## FIGURE LEGENDS

Figure 1. The  $\gamma 2$ (L287A) mutation reduces sensitivity to GABA but increases receptor efficacy in the presence of propofol. A & B, whole cell current traces induced by GABA in the absence and presence of 10  $\mu$ M PRO. The durations of GABA and PRO application are indicated by the bars above the current traces. C, comparison of the GABA concentration-response relationship in the absence and presence of 10  $\mu$ M PRO. In wild-type receptors, the GABA  $EC_{50}$  decreased from  $18.9 \pm 6.2$  to  $2.7 \pm 1.4$   $\mu$ M and the relative efficacy decreased from  $0.99 \pm 0.02$  to  $0.77 \pm 0.08$  in the presence of propofol. PRO had no significant effect on the Hill coefficient ( $1.83 \pm 0.05$  to  $2.03 \pm 0.23$ ) versus the WT-PRO condition. D, E & F, same as A, B & C but for mutant  $\alpha 1\beta 1\gamma 2$ (L287A) GABA<sub>A</sub> receptors. In mutant receptors, the GABA  $EC_{50}$  decreased from  $47.9 \pm 5.9$  to  $1.2 \pm 0.4$   $\mu$ M and the relative efficacy increased from  $1.00 \pm 0.01$  to  $1.76 \pm 0.22$  in the presence of PRO. PRO had no significant effect on the Hill coefficient ( $1.44 \pm 0.11$  to  $1.62 \pm 0.29$ ) versus the MUT-PRO condition. Significance was assessed at the  $p < 0.05$  level.  $4 \leq n \leq 5$ .

Figure 2. Propofol has no measurable effect on the intraburst kinetics of  $\alpha 1\beta 1\gamma 2$  GABA<sub>A</sub> receptor single-channel events. A, Single-channel openings recorded from a cell-attached patch. The GABA concentration in the electrode was 5 mM. B & C, Expanded time-scale views of a cluster (B) and a burst (C). The open-



closed idealizations of burst activity are shown above the current trace. D, E & F, same as A, B & C but for receptors in the presence of 5 mM GABA and 10  $\mu$ M PRO.

Figure 3. Propofol increases the intraburst  $P_o$  of  $\alpha 1\beta 1\gamma 2$ (L287A) GABA<sub>A</sub> receptor single-channel events. A, Single-channel openings recorded from a cell-attached patch. The GABA concentration in the electrode was 5 mM. B & C, expanded time-scale views of (B) clusters and (C) open-closed idealization of burst activity. D, E and F, same as A, B and C but for receptors in the presence of 10  $\mu$ M propofol.

Figure 4. Propofol increases the number of high- $P_o$  bursts in  $\alpha 1\beta 1\gamma 2$ (L287A) GABA<sub>A</sub> receptors but not in wild-type receptors. Binned data from multiple experiments were pooled in A, wild-type  $\alpha 1\beta 1\gamma 2$  and B, mutant  $\alpha 1\beta 1\gamma 2$ (L287A) GABA<sub>A</sub> receptors in the absence and presence of 10  $\mu$ M propofol. The normalized percentage of bursts showing burst  $P_o$  values  $\geq 0.70$  was: WT-PRO, 29%; WT-PRO, 26%; MUT-PRO, 8%; MUT+PRO, 87%.

Figure 5. Propofol had no measurable effect on the closed and open time components in wild-type receptors. In mutant receptors, propofol reduced the duration of one closed time component, increased the duration of two open components and introduced a third long-lived component. Histograms represent

binned data from representative patches containing wild-type (A & C) or mutant receptors (B & D). Dotted lines show the individual and summated components obtained by fitting the kinetic schemes shown in Figure 6A.

Figure 6. PRO increased the fractional occupancy of long-lived open states in mutant but not wild-type receptors. A, Kinetic schemes and rate constants ( $s^{-1}$ ) for the activation and modulation of wild-type  $\alpha 1\beta 1\gamma 2$  and mutant  $\alpha 1\beta 1\gamma 2(L287A)$  GABA<sub>A</sub> receptors. The schemes shown were used to idealize and fit data from each patch. The rate constants represent the global parameters from the fitting of pooled data. In the MUT-PRO condition, only two open states were required to adequately fit the data. B, comparison of the relative contribution of the 3 open states O1, O2 & O3 to channel activation obtained from intraburst dwell times. For the simulation of whole-cell dose response curves (see text), two sequential GABA binding steps were attached to C1. In wild-type receptors, PRO had no effects on the simulated GABA EC<sub>50</sub> (52.2 to 52.8  $\mu$ M in the absence and presence of PRO, respectively), relative efficacy (1.00 to 0.99), or Hill slope (1.46 to 1.46) versus the WT-PRO condition. In mutant receptors, PRO reduced the GABA EC<sub>50</sub> (73.8 to 16.2  $\mu$ M), increased the relative efficacy (1.00 to 2.29), and slightly increased the Hill slope (1.46 to 1.71) versus the MUT-PRO condition.

## TABLES AND TABLE LEGENDS

Mean single channel parameters for wild-type  $\alpha 1\beta 1\gamma 2$ s and mutant  $\alpha 1\beta 1\gamma 2$ s(L287A) receptors.

	Mean channel amplitude (pA)	Mean burst closed time (ms)	Mean burst open time (ms)	Mean burst $P_o$
WT-PRO	$1.75 \pm 0.05$	$1.71 \pm 0.19$	$2.35 \pm 0.31$	$0.54 \pm 0.03$
WT+PRO	$1.70 \pm 0.06$	$1.32 \pm 0.16$	$2.26 \pm 0.31$	$0.59 \pm 0.05$
MUT-PRO	$1.74 \pm 0.07$	$1.43 \pm 0.20$	$1.26 \pm 0.08^*$	$0.47 \pm 0.04$
MUT+PRO	$1.96 \pm 0.14$	$0.77 \pm 0.14^\dagger$	$7.32 \pm 2.07^\dagger$	$0.79 \pm 0.07^\dagger$

Table 1: PRO increased the mean single-channel burst open time and mean burst  $P_o$  only in mutant receptors. In the absence of PRO, mutant receptors had a higher mean burst closed time and lower mean burst  $P_o$  than wild-type receptors. In the presence of PRO, mutant receptors had the highest mean burst open time and mean burst  $P_o$  of the four conditions. The total numbers of patches for each condition were the following: WT-PRO, 7; WT+PRO, 6; MUT-PRO, 7; MUT+PRO, 8. Statistical significance is designated by: \*,  $p < 0.05$  vs. WT-PRO; †,  $p < 0.05$  vs. MUT-PRO.

Time constants and fractional areas for wild-type  $\alpha 1\beta 1\gamma 2s$  and mutant  $\alpha 1\beta 1\gamma 2s(L287A)$  receptors.

Time Constants, ms					
	$\tau_{C1}$	$\tau_{C2}$	$\tau_{O1}$	$\tau_{O2}$	$\tau_{O3}$
WT-PRO	$0.41 \pm 0.03$ (0.46)	$1.74 \pm 0.14$ (2.02)	$0.72 \pm 0.06$ (0.78)	$1.95 \pm 0.22$ (2.48)	$8.61 \pm 1.71$ (9.02)
WT+PRO	$0.47 \pm 0.08$ (0.41)	$1.73 \pm 0.14$ (1.81)	$0.64 \pm 0.06$ (0.69)	$1.91 \pm 0.14$ (2.18)	$6.10 \pm 0.54$ (7.12)
MUT-PRO	$0.46 \pm 0.05$ (0.56)	$1.91 \pm 0.24$ (2.50)	$0.69 \pm 0.07$ (0.84)	$2.01 \pm 0.14$ (2.11)	ND
MUT+PRO	$0.32 \pm 0.04$ (0.30)	$1.19 \pm 0.20^{\dagger}$ (1.27)	$1.14 \pm 0.15^{\dagger}$ (0.78)	$5.71 \pm 0.80^{\dagger}$ (4.94)	$24.97 \pm 2.63^{\dagger}$ (25.44)
Fractional Areas					
	$A_{C1}$	$A_{C2}$	$A_{O1}$	$A_{O2}$	$A_{O3}$
WT-PRO	$0.32 \pm 0.02$ (0.36)	$0.68 \pm 0.02$ (0.64)	$0.22 \pm 0.04$ (0.54)	$0.58 \pm 0.04$ (0.54)	$0.20 \pm 0.06$ (0.13)
WT+PRO	$0.37 \pm 0.07$ (0.38)	$0.63 \pm 0.07$ (0.62)	$0.17 \pm 0.05$ (0.27)	$0.68 \pm 0.04$ (0.61)	$0.15 \pm 0.05$ (0.12)
MUT-PRO	$0.31 \pm 0.02$ (0.34)	$0.69 \pm 0.02$ (0.66)	$0.53 \pm 0.08^*$ (0.71)	$0.47 \pm 0.08$ (0.29)	$0.00^*$

MUT+PRO	$0.38 \pm 0.05^{\dagger}$ (0.57)	$0.62 \pm 0.05$ (0.43)	$0.32 \pm 0.09$ (0.17)	$0.34 \pm 0.07^{\dagger}$ (0.27)	$0.34 \pm 0.13^{\dagger}$ (0.56)
---------	-------------------------------------	---------------------------	---------------------------	-------------------------------------	-------------------------------------

Table 2. PRO lengthened all three single-channel open time components in mutant receptors but not in wild-type receptors. Open time constants and fractional areas are reported as unweighted mean values  $\pm$  SEM, pooled from individual fits of each patch. Values from global fits of pooled data are shown in parentheses and are automatically weighted by the number of events detected for each component. When a component in the individual fit was missing compared to the global fit, the value was ignored and designated “ND” (for time constants) or treated as zero (for fractional areas) when calculating the mean values. PRO produced significant increases in the open time constants of mutant receptors, as well as an increase in the fractional area of the longest open time component ( $A_{O3}$ ). To a lesser extent, PRO also decreased the longer of the two closed time components ( $\tau_{C2}$ ) in mutant receptors. Under our single-channel recording and analysis conditions, PRO had no effect on wild-type receptors. Statistical significance is designated by: \*,  $p < 0.05$  vs. WT-PRO; †,  $p < 0.05$  vs. MUT-PRO.

Figure 1

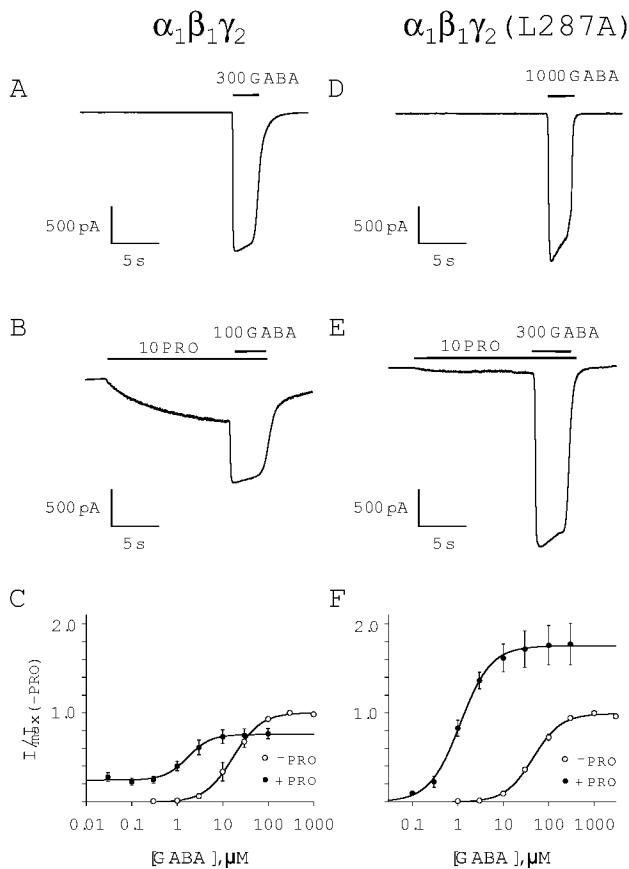


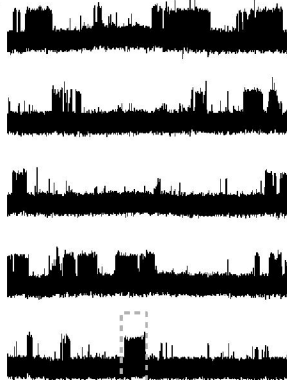
Figure 2

$\alpha_1\beta_1\gamma_2$

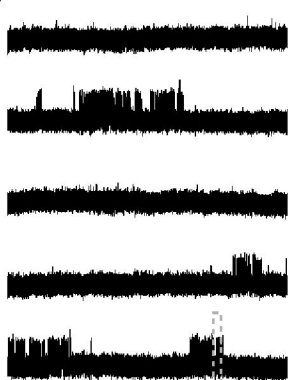
-PRO

+PRO

A



D



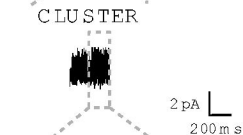
2 pA  
2 s

2 pA  
2 s

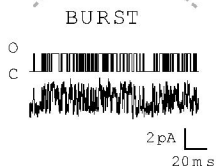
B



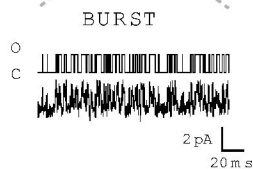
E



C



F

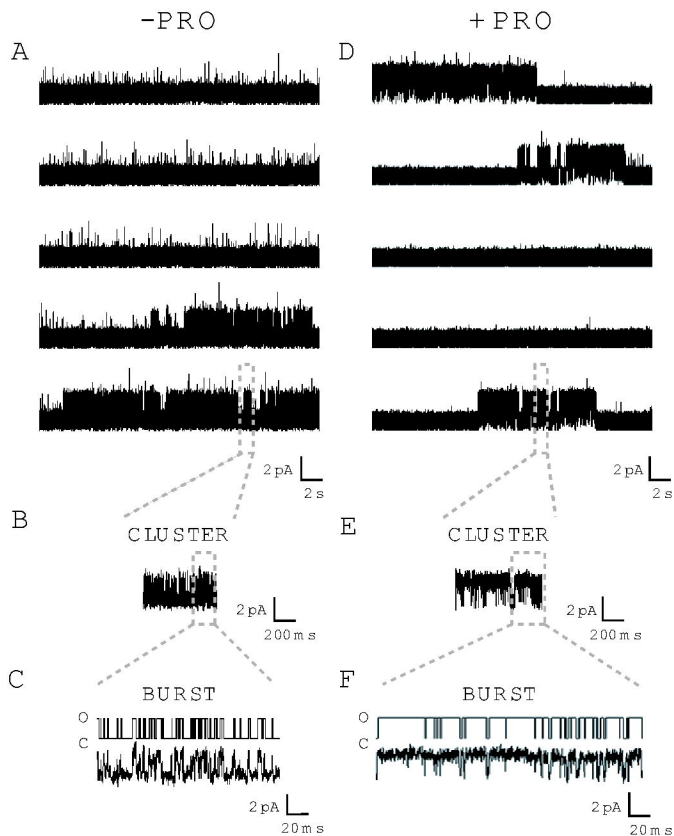


O  
C

O  
C

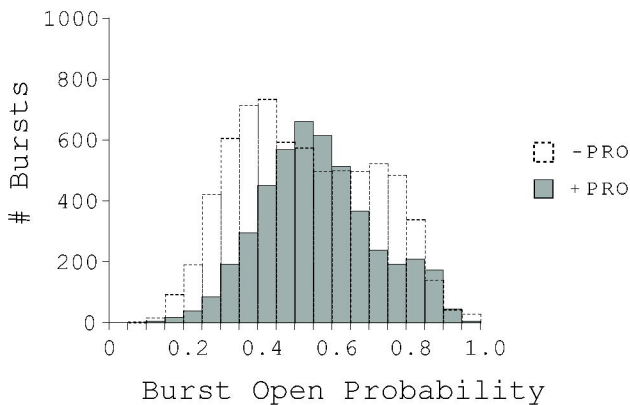
Figure 3

$\alpha_1\beta_1\gamma_2$  (L287A)





A

 $\alpha_1\beta_1\gamma_2$ 

B

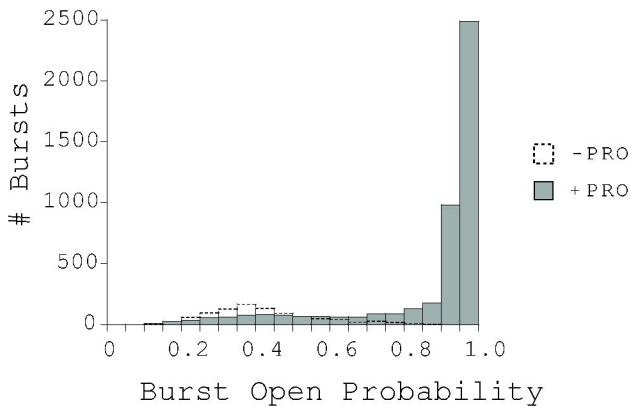
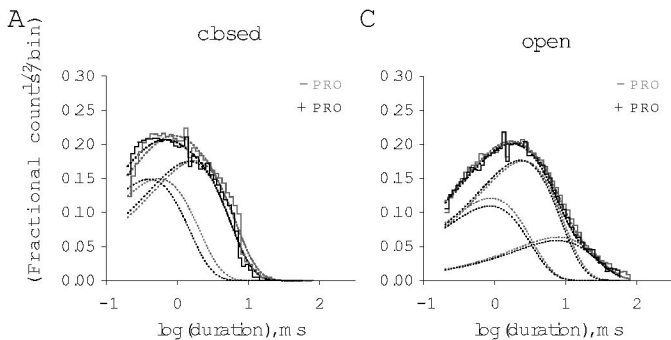
 $\alpha_1\beta_1\gamma_2$  (L287A)

Figure 5

$\alpha_1\beta_1\gamma_2$



$\alpha_1\beta_1\gamma_2$  (L287A)

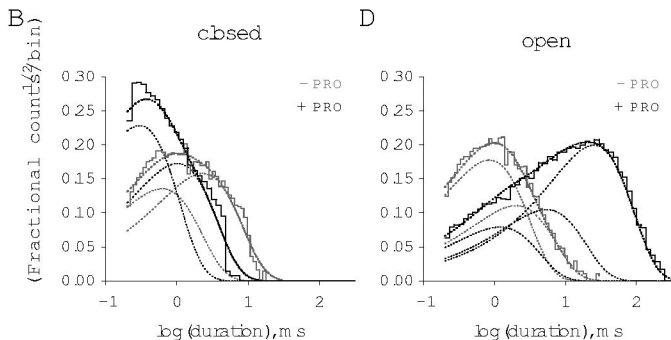
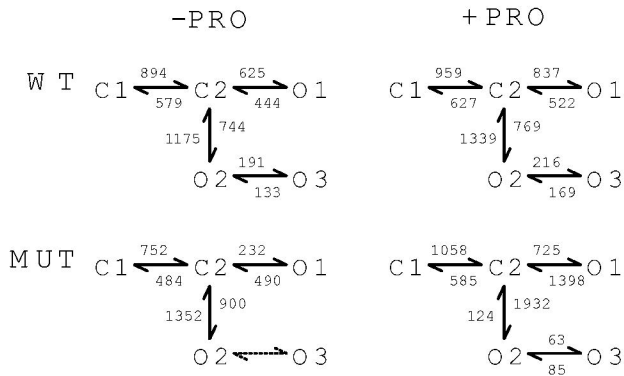


Figure 6

A



B

